JOURNAL OF CATALYSIS 132, 375–387 (1991)

Carbon Monoxide Adsorption by K/Co/Rh/Mo/Al_2O_3 Higher Alcohols Catalysts

ELAINE C. DECANIO AND DAVID A. STORM[1]

Texaco Research Center, P.O. Box 509, Beacon, New York 11258

Received June 11, 1990; revised July 2, 1991

The room temperature carbon monoxide adsorption characteristics of K/Co/Rh/Mo/Al_2O_3 catalysts are studied by chemisorption and FT–IR techniques. Most of the IR bands can be traced to those observed for Rh/Al_2O_3, K/Rh/Al_2O_3, and K/Rh(111). Several bands in the 1700–2000 cm^{-1} region become quite intense in these multicomponent catalysts when potassium loadings exceed 3 wt%. Significant intensity is observed only when all four elements are present with appropriate loadings. Studies with one-component precursors show: (1) the presence of Mo(0) in Mo/Al_2O_3 samples reduced at 673 K, (2) cobalt(+2) in octahedral positions on the alumina distinguishable from cobalt(+2) in particles of cobalt, and (3) the presence of a new band for Rh/Al_2O_3 at 2007 cm^{-1}. Studies with Rh/Mo/Al_2O_3 suggest Mo covers mainly the surfaces of the larger particles of Rh and forms a mixed oxide layer that does not chemisorb CO.

INTRODUCTION

In this work we use chemisorption and FT–IR techniques to investigate the room temperature carbon monoxide adsorption characteristics of K/Co/Rh/Mo/Al_2O_3 catalysts developed to make alcohols from synthesis gas (*1*). Although the main adsorption characteristics of Rh/Al_2O_3 (*2–9*), K/Rh(111) (*10*), Mo/Al_2O_3 (*11–14*), and Co/Al_2O_3 (*18–21*) have been reported, it was necessary to study the supported one-component samples in order to identify bands in multicomponent samples. Some new observations are reported for these single-component model catalysts.

Several groups of workers have studied *M*/Rh/SiO_2, where *M* is an oxophilic element (*22–26*). Apparently the element *M* forms a mixed metal oxide on the surfaces of the Rh particles (*22–26*). The analogous case of *M*/Rh/Al_2O_3 has received less attention (*26–28*). Some oxophilic elements have a strong interaction with the alumina, and the analogous covering of the rhodium by the oxophilic element may not occur (*26*). In this work we present evidence to show that molybdenum migrates during the reduction of the Rh/Mo/Al_2O_3 precursor and forms a mixed oxide mainly on the surfaces of the larger particles of rhodium.

EXPERIMENTAL

Sample Preparation

All samples were prepared by aqueous incipient wetness impregnation. The Al_2O_3 was Norton 6375: a γ alumina with a surface area of 216 m^2/g and a pore volume of 1.1 cc/g. The alumina pellets were ground to 20/40 mesh before impregnation. Ammonium heptamolybdate, rhodium nitrate, cobalt nitrate, and potassium carbonate were used for the impregnations. After impregnation, the Mo/Al_2O_3 samples were dried at 393 K for 16 h and then calcined in flowing air (60 cc/min) at 773 K for 3 h. The Co/Al_2O_3 samples and Rh/Al_2O_3 samples only were dried at 393 K for 16 h. The multicomponent samples, such as Rh/Mo/Al_2O_3 and Co/Rh/Mo/Al_2O_3, were prepared by impregnating calcined Mo/Al_2O_3 with rhodium or cobalt/rhodium solutions. These samples

[1] To whom correspondence should be addressed.

0021-9517/91 $3.00

were dried at 393 K for 16 h. The K/Co/Rh/Mo/Al_2O_3 catalysts were prepared by impregnating the dried Co/Rh/Mo/Al_2O_3 samples with potassium carbonate. Metal loadings in each sample are indicated by a number preceeding the element, i.e., 3Mo/Al_2O_3 represents a sample with 3 wt% molybdenum.

IR Studies

IR spectra were collected using a Nicolet 170 sx FT–IR spectrometer with a liquid-nitrogen-cooled MCT detector. All spectra were recorded after 100 scans with a resolution of 4 cm^{-1}. Spectra were measured using a quartz cell with NaCl windows attached to a glass gas handling/vacuum system. Hydrogen (ultrahigh purity) and carbon monoxide (99% purity) were passed through molecular sieve traps prior to use. A self-supporting wafer, 1.6 cm in diameter, was prepared by first grinding the sample to 325 mesh size, and then pressing 20 mg of the powder at 6000 psi. The wafers were mounted in the cell, evacuated for 12 h (10^{-5} Torr), and then reduced at 673 K in flowing hydrogen (60 cc/min) for 1 h. The reduced samples were evacuated at 673 K for 0.5 h and then cooled to room temperature. Unless noted otherwise, all IR spectra were measured after the reduced wafers had been first exposed to 100 Torr of CO for 0.5 h, and then evacuated for 0.5 h (5×10^{-5} Torr). All data manipulation was done using the Nicolet 660 computer. Curve analyses were carried out using the software supplied by Nicolet. The number and positions of some bands were determined by fitting the observed spectra with Gaussians. We find the characteristic bands for CO adsorbed on Rh/Al_2O_3 to be too broad to be fit by Lorentzians. This may reflect that each adsorption mode occurs in a variety of environments.

Volumetric Chemisorption

A conventional glass volumetric adsorption apparatus with a Texas Instruments pressure gauge and a turbo vacuum pump was used. The samples were reduced at 673 K with hydrogen for 3 h and then evacuated for 1 h (10^{-5} Torr). After cooling to room temperature, the samples were exposed to known amounts of CO. Total and reversible isotherms were measured at six pressures. The amounts chemisorbed were calculated by fitting straight lines to the two isotherms and then extrapolating these lines to zero pressure.

TABLE 1

Room Temperature Carbon Monoxide Chemisorption

Sample[a]	Uptake (cc/g)[b]	Uptake per atom
2Mo	0.04	0.01
3Mo	0.05	0.01
6Mo	0.13	0.01
9Mo	0.40	0.02
12Mo	0.60	0.02
0.7Co	0.07	0.03
2Co	0.15	0.02
0.5Rh	1.82	1.6
1Rh	3.45	1.6
1.5Rh	4.59	1.4
1Rh/3Mo	0.95	0.4(Rh)
1Rh/6Mo	0.56	0.2(Rh)
1Rh/12Mo	0.53	0.2(Rh)
0.7Co/1Rh/3Mo	1.65	—
2Co/1Rh/3Mo	1.24	—
0.5K/0.7Co/1Rh/3Mo	1.29	—
1.5K/0.7Co/1Rh/3Mo	0.94	—
3K/0.7Co/1Rh/3Mo	1.55	—
4.5K/0.7Co/1Rh/3Mo	1.25	—
6K/0.7Co/1Rh/3Mo	1.95	—

[a] Supported on alumina.
[b] Volume of carbon monoxide at 273 K.

RESULTS AND DISCUSSION

Mo/Al_2O_3

As shown in Table 1, only one to two CO molecules are adsorbed per hundred molybdenum atoms in the xMo/Al_2O_3 samples, where x = 2, 3, 6, 9, and 12. Consequently IR bands are not intense. Significant intensity has only been observed in the presence of CO and for samples with Mo loadings in the range of 8–12 wt% (*11–14*). As shown

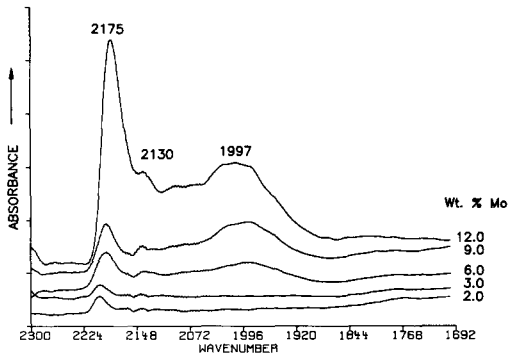

FIG. 1. Room temperature IR spectra of CO (20 Torr) adsorbed on Mo/Al_2O_3.

in Fig. 1, we observe the bands for a series of samples to vary systematically with molybdenum loading. A small band is observed at 2200 cm^{-1} for the $2Mo/Al_2O_3$ sample, and it ultimately shifts to 2175 cm^{-1} for the $12Mo/Al_2O_3$ sample. A small band at 2130 cm^{-1} is observed for all samples, and a broadband around 1997 cm^{-1} is observed for samples with molybdenum concentrations of 6 wt%, or more. The band at 2130 cm^{-1} is completely removed by evacuation, and those in the range of 2175–2200 cm^{-1} are diminished. The band around 1997 cm^{-1} is not significantly diminished by evacuation.

The strongest band has been observed at 2190 cm^{-1}, and it has been assigned to an adsorption by Mo(+5) or by a mixture of Mo(+5) and Mo(+4) (*11–14*). Peri observed this band to shift to lower wavenumbers in more reduced samples (*12*). XPS studies with these samples indicate that the $2Mo/Al_2O_3$ sample contains only Mo(+5), while the $12Mo/Al_2O_3$ sample contains a 2/1 mixture of Mo(+4) and Mo(+5) (*16*). The band at 2200 cm^{-1} is therefore assigned to an adsorption by Mo(+5), and so the adsorption by Mo(+4) must correspond to a band around 2175 cm^{-1}. Following Zaki *et al.*, the band at 2130 cm^{-1} is assigned to physical adsorption (*14*). The position of the new band around 1997 cm^{-1} suggests an adsorption by Mo(0). Peri reported bands around 2040 and 2025 cm^{-1} as corresponding to adsorption by Mo(0), but these bands vanished on evacuation (*12*). On exposing a sample of $Mo(CO)_6$, which had been adsorbed on dehydroxylated alumina and heated to temperatures high enough to decompose the $Mo(CO)_6$, Goldwasser *et al.* observed a band at 1989 cm^{-1} (*15*). We therefore assign the broadband around 1997 cm^{-1} to an adsorption by Mo(0). The presence of Mo(0) in samples of Mo/Al_2O_3 prepared by impregnation with ammonium heptamolydate, but reduced at high temperatures (1223 K), has been discussed recently by Chung *et al.* (*17*). Our work suggests that a very small amount of Mo(0) can be present even in samples that have been reduced at mild conditions (673 K for 1 h).

Co/Al_2O_3

The amounts of carbon monoxide chemisorbed by the 0.7 and 2 wt% samples of Co/Al_2O_3 are given in Table 1. These samples also chemisorb only a small amount of carbon monoxide: about 2 or 3 molecules per 100 cobalt atoms. The amount increases for the $2Co/Al_2O_3$ sample because some Co(0) is present, as discussed below, and because carbonates are observed to form by IR when the reduced sample is exposed to CO.

The IR spectra for adsorbed CO are shown in Fig. 2. A band, which vanishes on

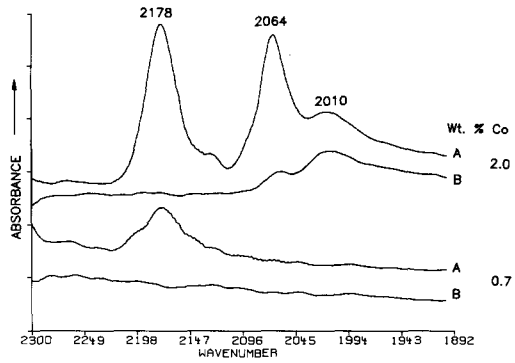

FIG. 2. Room temperature IR spectra of CO adsorbed on Co/Al_2O_3: A, 20 Torr; B, evacuated.

evacuation, is observed at 2178 cm^{-1} for both $0.7Co/Al_2O_3$ and $2Co/Al_2O_3$. Additional bands are observed for the $2Co/Al_2O_3$ sample around 2060 and 2010 cm^{-1}. Of these only the band at 2010 cm^{-1} is not diminished by evacuation.

Previous infrared studies have been with Co_3O_4, $CoAl_2O_4$, and $ZnCo_2O_4$ by Yao and Shelef (*18*); with calcined Co/Al_2O_3 by Ratnasamy and Knozinger (*19*); and with both calcined and sulfided Co/Al_2O_3 by Bachelier *et al.* (*20*). Only a single band was observed in the region 2178–2185 cm^{-1}. Since only Co(+2)-ions in octahedral positions adsorb, these bands were assigned to Co(+2)-ions in octahedral positions on the alumina, or surface ions associated with Co_3O_4 particles (*19, 20*). Topsøe and Topsøe showed that the octahedral holes on alumina are filled for loadings around 2 wt% (*21*). Particles of Co_3O_4 then form when samples are calcined (*21*). The samples in this work were not calcined, and so it is unlikely that particles of Co_3O_4 formed. Nevertheless, particles containing several cobalt atoms should form during reduction when the holes are filled. The band at 2178 cm^{-1} is therefore assigned to Co(+2)-ions located in octahedral holes on the alumina, while the bands at 2064 and 2010 cm^{-1} are assigned to carbon monoxide adsorbed on particles. The band at 2064 cm^{-1} can be diminished by evacuation, so it must correspond to adsorption by an ionic form of cobalt, i.e., cobalt in octahedral positions on the surfaces of partially reduced particles. The band at 2010 cm^{-1} remains on evacuation, and it is assigned to an adsorption by metallic cobalt. For the discussion of $Co/Rh/Mo/Al_2O_3$ below, it is useful to note that there is a decrease in the more basic hydroxyls when cobalt is supported on the alumina.

Rh/Al_2O_3

The amounts of carbon monoxide chemisorbed by the reduced Rh/Al_2O_3 samples are also given in Table 1; corresponding IR spectra are shown in Fig. 3. On a weight basis the $1Rh/Al_2O_3$ sample chemisorbs 50 times more carbon monoxide than $3Mo/Al_2O_3$ or $0.7Co/Al_2O_3$. The $0.5Rh/Al_2O_3$ and $1Rh/Al_2O_3$ samples are well-dispersed with CO/Rh ratios of 1.6.

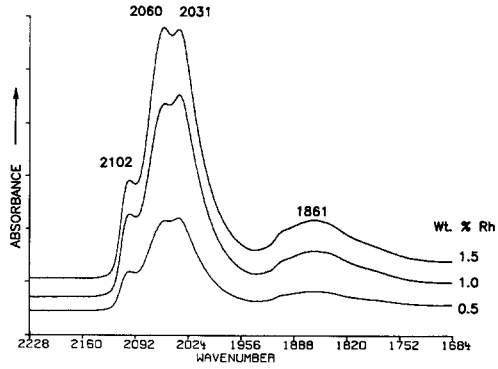

FIG. 3. Room temperature IR spectra of CO adsorbed on Rh/Al_2O_3.

Several groups of workers have studied Rh/Al_2O_3 (*2–9*). Bands at 2100 and 2031 cm^{-1} have been assigned to a Rh(I)–gem dicarbonyl(*2–9*). These bands are not coverage-dependent, and they are the only bands observed with very well-dispersed Rh/Al_2O_3 (*4*). Furthermore EXAFS studies have shown that the very well-dispersed phase is involved in this adsorption (*7*). Basu *et al.* have shown that these very small particles are oxidized during adsorption by the basic hydroxyls on the alumina (*9*).

The band around 2060 cm^{-1} has been assigned to a linear Rh(0)–carbonyl, and the broadband around 1860 cm^{-1} has been assigned to a bridging carbonyl (*2, 4, 5*). Since these bands are observed in less well-dispersed samples, and their positions are coverage-dependent, these sites are thought to be on larger particles. On analyzing the asymmetry in intensity of the two bands corresponding to the gem dicarbonyl, Rice *et al.* suggested that there might be a band near 2000 cm^{-1} (*5*). Such asymmetry would also occur if the angle between the two CO molecules in the gem dicarbonyl were greater than 90°; but the asymmetry depended on

loading in their work (*5*), and they argued that it was unreasonable to expect the angle to change significantly with dispersion (*5*).

All of these features are observed in Fig. 3, and the parameters are given in Table 2. The position of the linear carbonyl shifts 6–7 cm^{-1} higher when the samples are exposed to 20 Torr of carbon monoxide, while those for the gem dicarbonyl do not shift. The ratios of intensities for the gem and linear carbonyls are approximately 1 for the 0.5 and 1.0 wt% rhodium samples, and 0.88 for the 1.5 wt% sample, reflecting a lower dispersion with increasing Rh loading. This is consistent with the chemisorption results given in Table 1 that show that the 0.5 wt% sample and the 1.0 wt% sample correspond to a CO/Rh of 1.6, while that for the 1.5 wt% is 1.4.

In order to obtain more detailed information, the 1900–2200 cm^{-1} region was fitted with Gaussian peaks. Fit spectra are shown in Fig. 4, and peak positions, widths, and intensities are given in Table 2. The computer analysis reveals a band at 2007 cm^{-1} with a width somewhat larger than that for the linear carbonyl. Note that the trailing edge of the envelope shown in Fig. 4 cannot be matched if this band is not included. The position and intensity of the band at 2007 cm^{-1} relative to that for the gem dicarbonyl does not change with loading. Also, the 2007 cm^{-1} band does not shift with CO coverage. The relative intensity of this band to that for the gem dicarbonyl is also constant in the three samples. This could mean that the 2007 cm^{-1} band is really associated with the gem dicarbonyl in some manner. However, as we show below, the intensity of this band is decoupled from that of the gem dicarbonyl in samples containing Mo; Mo and Co; and K, Mo, and Co. Consequently we believe it corresponds to a separate adsorption site.

Rh/Mo/Al_2O_3

The amounts of carbon monoxide chemisorbed by reduced samples of 1Rh/*x*Mo/Al_2O_3 with x = 3, 6, and 12 wt% are given in Table 1. Supporting rhodium on 3Mo/Al_2O_3 (calcined) reduces the chemisorption capacity of rhodium by a factor of 4. This is surprising when one considers that molybdenum covers only about one-third of the alumina area in the Mo/Al_2O_3 precursor. The chemisorption is reduced by a factor of 8 if 6Mo/Al_2O_3 is used as the support, and it decreases a small amount more if 12Mo/Al_2O_3 is used.

Paralleling these chemisorption results, the intensities of the linear and bridging carbonyls, shown in Fig. 5, are reduced in 1Rh/3Mo/Al_2O_3 when compared to 1Rh/Al_2O_3. The intensities of the bands for the gem dicarbonyl are not reduced, however. The band for the linear carbonyl also shifts by 7 cm^{-1} to higher wavenumbers, and the band for the bridging shifts 18 cm^{-1} higher. The bands for the gem dicarbonyl do not shift. The band at 2007 cm^{-1} also does not shift, but its intensity decreases by a factor of 2 relative to that for the gem dicarbonyl.

When compared to 1Rh/3Mo/Al_2O_3, there is an additional decrease in both chemisorption capacity and intensities when 6Mo/Al_2O_3 is the support. The linear carbonyl does not shift from its position in 1Rh/3Mo/Al_2O_3, but the bridging carbonyl shifts an additional 20 cm^{-1} higher. The position of the bands for the gem dicarbonyl and the band at 2007 cm^{-1} are the same as in 1Rh/Al_2O_3. Although the total IR intensity has decreased, the ratio of intensity for the gem dicarbonyl to that for the linear carbonyl is higher. The intensity of the band at 2007 cm^{-1} is also higher relative to that for the gem dicarbonyl. Increasing the Mo loading to 12 wt% causes only a small decrease in chemisorption capacity and IR intensity. The intensity for the band at 2007 cm^{-1} increases relative to that for the gem dicarbonyl.

Rh/X/Al_2O_3 has not received as much attention as Rh/X/SiO_2, where X represents a oxophilic element (*22–34*). In general, authors report a suppression in chemisorption capacity, and for the silica cases, a reduc-

TABLE 2

IR Spectral Parameter for 1900–2200 cm^{-1} Region

Sample[a]	Position (cm^{-1})	Intensity	Width (cm^{-1})	R^b	R^c
0.5Rh	2101	0.082	24.3	1.0	0.46
	2060	0.199	42.0		
	2031	0.144	20.0		
	2007	0.090	50.0		
1Rh	2101	0.160	21.0	1.0	0.42
	2060	0.405	39.4		
	2031	0.255	28.0		
	2008	0.165	50.0		
1.5Rh	2102	0.195	21.0	0.9	0.40
	2060	0.560	42.0		
	2031	0.300	27.0		
	2008	0.210	50.0		
1Rh/3Mo	2103	0.260	21.0	2.5	0.20
	2068	0.235	43.0		
	2034	0.320	30.0		
	2007	0.114	48.0		
1Rh/6Mo	2103	0.155	21.0	2.8	0.24
	2068	0.135	43.0		
	2037	0.225	31.0		
	2007	0.090	46.0		
1Rh/12Mo	2103	0.088	21.0	2.8	0.28
	2067	0.075	43.0		
	2037	0.120	31.0		
	2009	0.060	55.0		
0.7Co/1Rh/3Mo	2100	0.110	21.0	1.5	0.39
	2063	0.190	42.0		
	2033	0.170	30.0		
	2007	0.110	48.0		
2Co/1Rh/3Mo	2102	0.130	20.0	2.6	0.33
	2068	0.110	48.0		
	2033	0.170	30.0		
	2008	0.095	48.0		
0.5K/0.7Co/1Rh/3Mo	2098	0.130	18.5	1.5	0.30
	2063	0.207	45.0		
	2029	0.187	32.0		
	2003	0.095	55.0		
1.5K/0.7Co/1Rh/3Mo	2095	0.061	18.5	1.0	0.66
	2057	0.143	45.0		
	2026	0.076	32.0		
	2003	0.091	55.0		
	1952	0.037	60.0		
	1894	0.027	60.0		
4.5K/0.7Co/1Rh/3Mo	2090	0.009	18.5	0.2	4.0
	2041	0.113	42.0		
	2027	0.010	32.0		
	2000	0.076	65.0		
	1940	0.066	48.0		
	1896	0.060	55.0		
	1849	0.016	25.0		

[a] Supported on Al_2O_3.

[b] Intensity ratio of gem dicarbonyl to linear carbonyl.

[c] Intensity ratio of band at 2007 cm^{-1} to gem dicarbonyl.

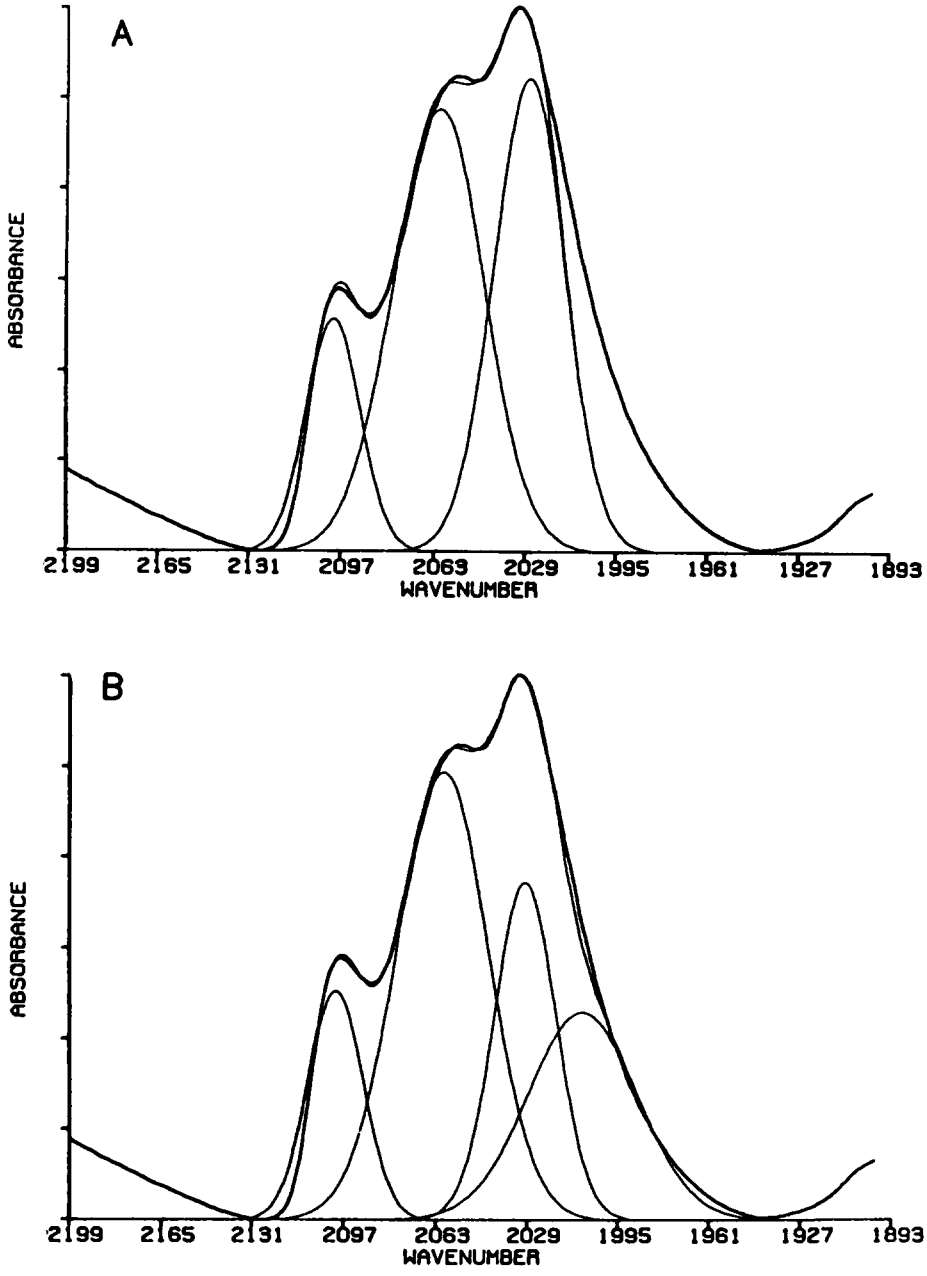

FIG. 4. Fitted Spectra for 1Rh/Al_2O_3: A, 5 G; B, 4 G. Dark curve represents data; light curves are fits.

tion in intensities for both the linear and bridging carbonyls and a constant intensity for the gem dicarbonyl. In many cases the linear and bridging carbonyls shift to lower wavenumbers (*29–33*). Kip *et al.* report similar behavior for Rh/V/Al_2O_3, but believe vanadium only interacts with rhodium during a high-temperature calcination (*26*). Sudhakar *et al.* reported a decrease in chemisorption capacity for 3Rh/7.5Mo/Al_2O_3 (*27*). More recently Foley *et al.* observed rhodium–molybdenum particles in Rh/Mo/

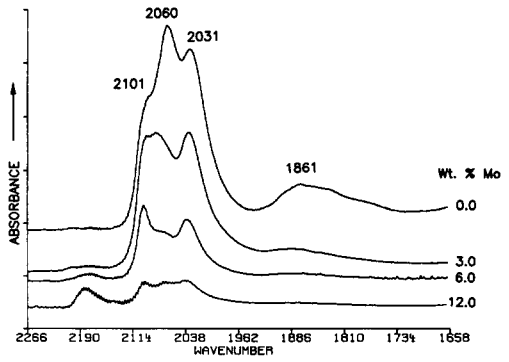

FIG. 5. Room temperature IR spectra of CO adsorbed on $1Rh/Mo/Al_2O_3$ as a function of Mo loading.

Al_2O_3 catalysts prepared by a sequential adsorption of the metal carbonyls (*28*).

It is evident that many combinations of rhodium with an oxophilic element on silica have characteristics similar to those in this study. Wilson *et al.* (*22*), Kip *et al.* (*26*), and van den Berg *et al.* (*23*) attribute these effects to the oxophilic element forming a mixed metal oxide surface layer on the rhodium particles. Since Mo/Al_2O_3 (calcined) was simply impregnated with rhodium nitrate, dried, and reduced in this work, we can rule out compound formation before reduction. Our observations therefore suggest that molybdenum migrates during the reduction step mainly to the larger particles of rhodium and forms a mixed oxide surface layer that does not chemisorb carbon monoxide.

Work with Rh/Al_2O_3 (*2–9*) indicates that the bands for the linear and bridging carbonyls are associated with the larger particles of Rh(0), while those for the gem dicarbonyl are associated with very small particles of Rh. The ratio of intensity for the gem dicarbonyl to that for the linear carbonyl is thus a measure of the number of sites associated with small particles compared to the number associated with large particles. When making this argument, however, one must take into account the extinction coefficients for the two modes of absorption. The extinction coefficient is larger for the gem dicarbonyl (*3, 4*), and so the intensity for the gem dicarbonyl should be more sensitive to changes in site density. In this case, however, the intensity for the gem dicarbonyl in $1Rh/3Mo/Al_2O_3$ is the same as that in $1Rh/Al_2O_3$, while the intensities for the linear and bridging carbonyls are smaller. This indicates a decrease in the number of sites on larger particles. One could argue that the extinction coefficients changed, but it is difficult to explain such a change if molybdenum is not interacting more with the larger particles. The explanation that molybdenum disperses the rhodium (*34*) is ruled out because the chemisorption capacity decreases. One would expect the newly created small particles to adsorb two molecules of CO per rhodium atom. It is possible that some gem dicarbonyl forms by a reductive carbonylation of Rh(III), with CO_2 as the by-product (*35*), but we observe no change in the carbonate region when the spectrum is compared to that for Rh/Al_2O_3.

Further evidence that the molybdenum interacts with mainly the larger particles of rhodium is provided by the shift in the position of the linear and bridging carbonyls. Although the shifts in the linear and bridging carbonyls are opposite to those observed in the SiO_2 cases (*29–33*), the shift is consistent with adsorption by more oxidized particles of rhodium. Rice *et al.* (*5*) observed a similar shift of the linear carbonyl after a $10Rh/Al_2O_3$ sample had been exposed to oxygen at room temperature. One could speculate that molybdenum oxidizes the rhodium. Since the well-dispersed rhodium phase is more resistant to oxidation than the large particles (*2, 4*), it is reasonable, therefore, that the larger particles are more affected by the molybdenum.

Molybdenum must also interact with the site giving rise to the band at 2007 cm^{-1}. The band does not shift, but its intensity, relative to that for the gem dicarbonyl, is smaller in $1Rh/3Mo/Al_2O_3$ than $1Rh/Al_2O_3$, but larger in $1Rh/6Mo/Al_2O_3$ and $1Rh/12Mo/Al_2O_3$ because the intensity for the gem dicarbonyl decreases. This is one indi-

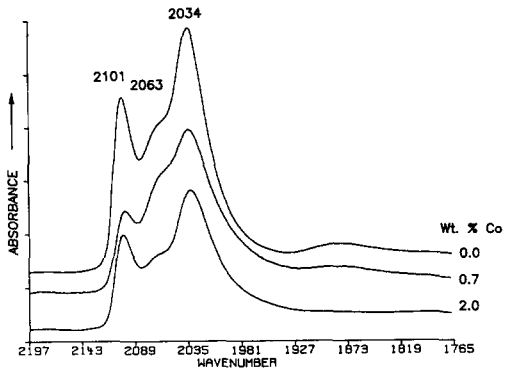

FIG. 6. Room temperature IR spectra of CO adsorbed on Co/1Rh/3Mo/Al_2O_3 as a function of Co loading.

cation that the site associated with this band is independent of the sites that give the gem dicarbonyl.

Co/Rh/Mo/Al_2O_3

The amounts of carbon monoxide chemisorbed by the 0.7Co/1Rh/3Mo/Al_2O_3 and the 2Co/1Rh/3Mo/Al_2O_3 samples are given in Table 1. The addition of cobalt to the Rh(1)/Mo(3)/AlO_3 precursor increases the chemisorption capacity by about 70%. We attribute this, however, to carbonate formation, observed by IR.

The 1800–2200 cm^{-1} region is shown in Fig. 6. Parameters for the fitted spectra are given in Table 2. These data indicate that cobalt has a very small effect on the bands for Rh/Mo/Al_2O_3. The intensity of the gem dicarbonyl decreases relative to the 2007 cm^{-1} band in the 0.7 wt% sample, again indicating these two bands are decoupled. The decrease in intensity of the gem dicarbonyl can be explained by a decrease in the number of basic hydroxyls, which is observed by IR. As discussed in the section on Co/Al_2O_3, cobalt addition decreases the intensity for the more basic hydroxyls. The intensities of both the linear and bridging carbonyls and the new band decrease relative to that for the gem dicarbonyl in the 2 wt% sample. Perhaps there is a weak cobalt–rhodium interaction, similar to the molybdenum–rhodium interaction discussed above, which occurs when the octahedral holes on the alumina are filled, and more mobile cobalt becomes available during reduction. The main point, however, is that cobalt has a very small effect on the rhodium character of Rh/Mo/Al_2O_3 sample.

K/Co/Rh/Mo/Al_2O_3

The chemisorption results for the xK/0.7Co/1Rh/3Mo/Al_2O_3 catalysts, where x = 0, 0.5, 1.5, 3.0, 4.5, and 6.0, are given in Table 1, and the spectra are shown in Fig. 7. Parameters for the fitted spectra are given in Table 2. Both the IR and chemisorption data suggest a change in the nature of the surface for potassium loadings greater than 1.5 wt%. The catalyst is rhodium-like in its CO adsorption characteristics for 0–1.5 wt% potassium, but new bands appear with greater loadings (Fig. 7). Similarly, the downward trend in the chemisorption capacity is reversed when the loading exceeds 1.5 wt%. As discussed below, there is a systematic decrease in the intensity of the gem dicarbonyl with potassium in the range of 0–3 wt%. This adsorption mode is essentially extinguished in the sample containing 3 wt% potassium; and since this mode accounts for two CO molecules per site, chemisorption capacity decreases. The chemisorption capacity begins to increase for higher potassium loadings because a significant amount of carbonates form on the

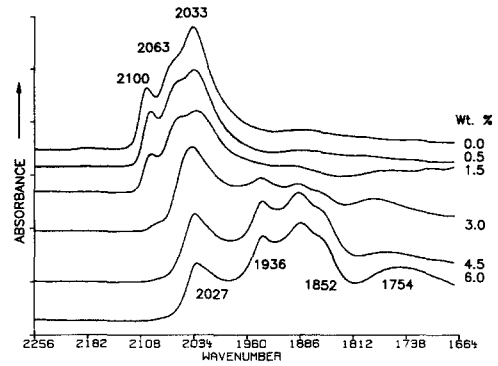

FIG. 7. Room temperature IR spectra of CO adsorbed on K/0.7Co/1Rh/3Mo/Al_2O_3 as a function of K loading.

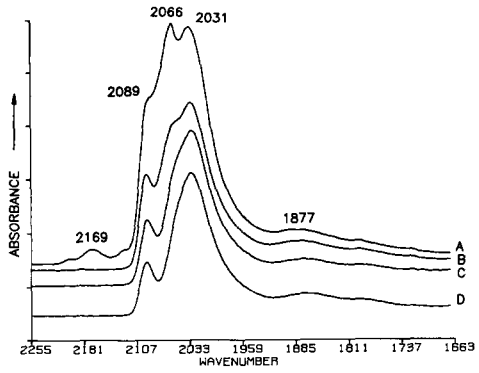

FIG. 8. IR spectra of CO adsorbed on 0.5K/0.7CO/1Rh/3Mo/Al_2O_3 at different coverages: A, room temperature, 20 Torr CO; B, room temperature after evacuation; C, 373 K after evacuation; D, room temperature after evacuation at 373 K.

alumina and because new bands appear, which may indicate new sites.

It is convenient to consider the 2000–2200 cm^{-1} region first. Figure 7 and the data in Table 2 show the decrease in intensity of the gem dicarbonyl with increasing potassium loading. A similar, but smaller, effect has been observed by Blackmond *et al.* (*36*) and by Kesraoui *et al.* (*37*) with Cs/Rh/Al_2O_3, and by Angevaare *et al.* (*38*) with K/Rh/SiO_2. These authors suggest that the alkali atom interacts with the sites that adsorb as the gem dicarbonyl. This may be true, but we also note that potassium reacts with the remaining basic hydroxyls on the alumina, and so part, if not all, of the decrease in intensity for the gem dicarbonyl can be attributed to the decrease in the number of basic hydroxyls needed to form the gem dicarbonyl. The shift in the position of the gem dicarbonyl does suggest a direct interaction between the potassium and the well-dispersed rhodium phase, however. It is striking that only 0.5 wt% potassium has this effect when, as discussed above, larger amounts of molybdenum and cobalt only shift the bands for the linear and bridging carbonyls.

An examination of the linear band (Fig. 7 and the data in Table 2) indicates a systematic decrease in intensity and position with increasing potassium loading. Angevaare *et al.* (*38*) observed a similar effect for K/Rh/SiO_2. By doing coverage-dependent experiments, these authors deduced that the shift is due to a decrease in the dipole–dipole interactions between adsorbed carbon monoxide molecules (*38*). They suggest that potassium dilutes the adsorbed CO layer (*38*). Figure 8 shows that this band for the linear carbonyl is coverage-dependent; it shifts by about 30 cm^{-1} as the CO coverage is changed from that corresponding to an exposure to 20 Torr to that corresponding to evacuation at 373 K. The total shift of this band between 0 and 6 wt%-potassium is also about 30 cm^{-1}. These shifts are close to those observed by Angevaare *et al.* (*38*). Thus it appears that the shift of the linear band is due to a change in coverage. The cause of the dilution is not clear except, as discussed below, new bands appear that may correspond to sites removed from the larger particles of reduced rhodium.

The spectra in the 1700–2000 cm^{-1} region for samples with potassium loadings of 0.5, 3, and 6 wt% are shown in Figs. 8, 9 and 10, respectively. As illustrated in Fig. 7, several significant new bands appear with increasing potassium loading. These bands are not

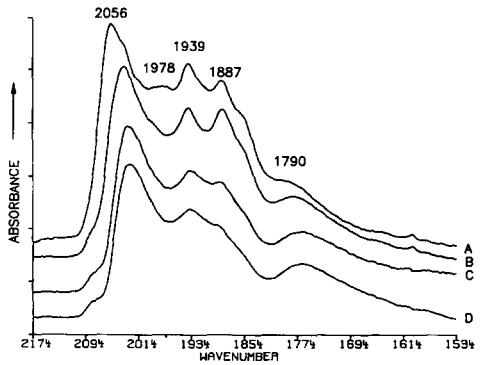

FIG. 9. IR spectra of CO adsorbed on 3K/0.7Co/1Rh/3Mo/Al_2O_3 at Different Coverages: A, room temperature, 20 Torr CO; B, room temperature after evacuation; C, 373 K after evacuation; D, room temperature after evacuation at 373 K.

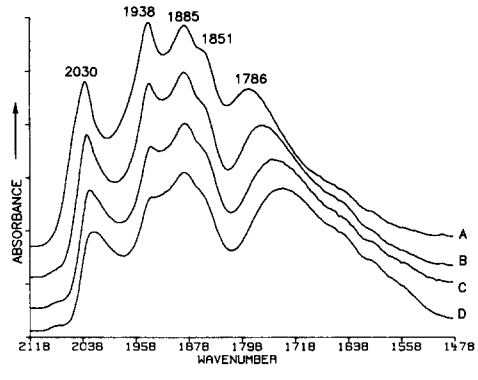

FIG. 10. IR spectra of CO adsorbed on 6K/0.7Co/1Rh/3Mo/Al_2O_3 at different coverages: A, room temperature, 20 Torr CO; B, room temperature after evacuation; C, 373 K after evacuation; D, room temperature after evacuation at 373 K.

easily related to those in the precursors, as illustrated by Fig. 11.

The spectra shown in Figs. 8, 9, and 10 correspond to coverage-dependent experiments. Spectrum A in each figure was measured after a freshly reduced sample was exposed to 20 Torr of carbon monoxide at room temperature. The samples were then successively evacuated at room temperature and at 373 K, recording spectra B and C, respectively. The samples were then cooled to room temperature, and Spectra D were recorded. The changes observed in Figs. 8–10 are reversible. Spectra A are recovered by reexposing the samples to 20 Torr of carbon monoxide at room temperature.

Consider the band at 1790 cm^{-1}, which is most apparent in Figs. 9 and 10. This band also appears in the spectra for K/Rh/Al_2O_3 for high potassium loading (Fig. 11). As shown in Figs. 9 and 10, this band shifts to lower wavenumbers with decreasing CO coverage. Also it shifts to lower wavenumbers with increasing potassium loading. These observations are in agreement with those made by Crowell and Somorjai (*10*) with K/Rh(111). These authors observe a coverage-dependent band in the region 1530–1855 cm^{-1} that shifts lower with increasing potassium concentration and lower with decreasing CO coverage. A band around 1750 cm^{-1} also appears to be present in the spectra published by Blackmond *et al.* (*38*) for Cs/Rh/Al_2O_3 and by Angevaare *et al.* (*38*) for K/Rh/SiO_2. We note that Uram *et al.* (*39*) also observe a band at 1750 cm^{-1} for CO adsorbed on K/Ni(111), which they assigned to local CO anionic complexes with potassium. We observe the intensity of the 1750 cm^{-1} band to depend on rhodium loading, and so we suggest that this band corresponds to CO complexes with potassium located on the rhodium surface. The formation of complexes might explain the decrease of CO in the vicinity of the linear sites.

The bridging carbonyl appears around 1870–1880 cm^{-1} in Fig. 8. This band either remains around 1880 cm^{-1}, as in Figs. 9 and 10, or shifts down to about 1860 cm^{-1} with increasing potassium loading. In any case its intensity is considerably enhanced by potassium in these multicomponent catalysts. On the basis of the fact that the linear carbonyl shifts to lower wavenumbers with increasing potassium and the band around 1850 cm^{-1} is coverage-dependent, we assign the 1850 cm^{-1} band in Figs. 9 and 10 to the bridging carbonyl. This assignment to a rhodium site is consistent with other work;

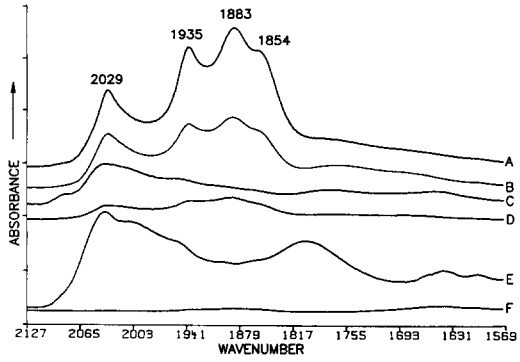

FIG. 11. Room temperature IR spectra of CO adsorbed on one-, two-, and three-component samples: A, 4.5K/2Co/1Rh/3Mo/Al_2O_3; B, 4.5K/0.7Co/1Rh/3Mo/Al_2O_3; C, 4.5K/1Rh/3Mo/Al_2O_3; D, 4.5K/0.7Co/3Mo/Al_2O_3; E, 4.5K/1Rh/Al_2O_3; F, 4.5K/0.7Co/Al_2O_3.

Angevaare *et al.* (*38*) report a small band around 1825 cm^{-1} for $K/Rh/SiO_2$, and Solymosi *et al.* (*40*) report a weak band around 1850 cm^{-1} for $K/Rh/Al_2O_3$.

Unfortunately we are not able to assign the new band around 1880 cm^{-1} in Figs. 9 and 10 at this time. A band at this position has not been reported; and it is not apparent in the spectra for any of the one-, two-, or three-component precursors shown in Fig. 11. We note this band is not coverage-dependent, which may indicate an isolated site.

The band around 1940 cm^{-1}, shown in Figs. 9 and 10, is also not apparent in the spectra for the $0.5K/0.7Co/1Rh/3Mo/Al_2O_3$ sample (Fig. 8) or in the spectra for any of the precursors shown in Fig. 11. However, on magnification of the region between 2030 and 1850 cm^{-1} in the spectra for $K/Rh/Al_2O_3$, this band appears to grow out of the background with increasing potassium loading. It does not shift very much with changes in potassium loading or CO coverage. Possibly this band corresponds to a linear carbonyl in which the CO interacts with potassium.

Finally, as discussed above, the positions and intensities of the IR bands in the 1700–2000 cm^{-1} region depend strongly on potassium loading (Fig. 7). The intensities of these bands are also affected by molybdenum and cobalt loading, as shown in Fig. 11. Molybdenum is necessary to have significant intensity in this region, but more than 3 wt% causes a decrease in intensity. The results for $Rh/Mo/Al_2O_3$, discussed above, suggest that this is because molybdenum migrates during the reduction step and covers the rhodium particles, thereby decreasing intensities. In contrast, these bands become more intense with increasing cobalt loading. The study of Co/Al_2O_3, discussed above, suggests that mobile cobalt will become available at higher loadings to interact with these sites, but the comparison with the $Co/Rh/Mo/Al_2O_3$ study, discussed above, shows that potassium is also needed to promote this interaction.

SUMMARY

Chemisorption and FT–IR techniques are used to relate the CO adsorption characteristics for $K/Co/Rh/Mo/Al_2O_3$ higher alcohol catalysts to those of the one-, two-, and three-component precursors. Most of the bands can be traced to those for Rh/Al_2O_3 and $K/Rh/Al_2O_3$. The bands for the gem dicarbonyl, very promenent in spectra for Rh/Al_2O_3, are extinguished by potassium in these multicomponent catalysts. The linear and bridging carbonyl bands, also prominent features, are shifted down somewhat. Actually these bands are shifted higher by an interaction between rhodium and molybdenum in $Rh/Mo/Al_2O_3$ and then lower by the combined interaction in the multicomponent catalysts, so that they end up only somewhat lower than in Rh/Al_2O_3. The band for the bridging carbonyl is enhanced by appropriate amounts of Mo, Co, and K. Also, several bands in the 1700–2000 cm^{-1} region, which are apparently hidden in the background for $K/Rh/Al_2O_3$, become more intense in the multicomponent catalysts when Mo, Co, and K have appropriate loadings. A band around 1940 cm^{-1} is assigned to a linear carbonyl in which the CO interacts with potassium. A band around 1750 cm^{-1} is assigned to anionic complexes of CO with potassium. A band around 1890 cm^{-1} is unassigned.

Studies with one-component precursors reveal new features. A band around 2000 cm^{-1} is observed in reduced samples of Mo/Al_2O_3 with molybdenum loadings greater than 6 wt%. On the basis of the work of Goldwasser *et al.* (*15*), we suggest that this band indicates that a small amount of Mo(0) can be present in samples reduced under mild conditions. Bands at 2200 cm^{-1} and 2175 cm^{-1} are assigned to adsorptions by Mo(+5) and Mo(+4), respectively. Additionally we find that Co(+2) in octahedral positions on the alumina produces a band at 2178 cm^{-1}, while Co(+2) in particles produces a band at 2160 cm^{-1}. Careful curve analysis of the spectra for Rh/Al_2O_3 reveal a band at 2007 cm^{-1}, which is unassigned.

Studies with Rh/Mo/Al_2O_3 suggest that molybdenum migrates during the reduction and covers mainly the surfaces of the larger particles of rhodium to form a phase that does not chemisorb CO. The gem dicarbonyl is unaffected when molybdenum loadings are less than 3 wt%, but the linear and bridging carbonyls suffer a loss in intensity and they are shifted to higher wavenumbers. It appears that the molybdenum oxidizes the Rh(0), and since the well-dispersed phase is more resistant to oxidation (*2, 4*), molybdenum tends to interact mainly with the larger particles.

REFERENCES

1. Wong, S. F., Storm, D. A., and Patel, M. S., US Patents 4,980,380 and 4,983,638.
2. Yang, A. C., and Garland, C. W., *J. Phys. Chem.* **61,** 1504 (1957).
3. Duncan, T. M., Yates, J. T., Jr., and Vaughan, R. W., *J. Chem. Phys.* **73,** 975 (1980).
4. Cavanagh, R. R., and Yates, J. T., Jr., *J. Chem. Phys.* **74,** 150 (1981).
5. Rice, C. A., Worley, S. D., Curtis, C. W., Guin, J. A., and Tarrer, A. R., *J. Chem. Phys.* **74,** 6487 (1981).
6. Yates, J. T., Jr., and Kolasinski, K., *J. Chem. Phys.* **79,** 1026 (1983).
7. Van't Bilk, H. F. J., Van Zon, J. B. A. D., Hulzinga, T., Vis, J. C., Koningsberger, D. C., and Prins, R., *J. Phys. Chem.* **87,** 2264 (1983).
8. Solymosi F., and Pasztor, M., *J. Phys. Chem.* **89,** 4789 (1985).
9. Basu, P., Panayotov, D., and Yates, J. T., Jr., *J. Phys. Chem.* **91,** 3133 (1987).
10. Crowell, J. E., and Somorjai, G. A., *Appl. Surf. Sci.* **19,** 73 (1984).
11. Millman, W. S., Crespin, M., Cirillo, A. C., Jr., Abdo, S., and Hall, W. K., *J. Catal.* **60,** 404 (1979).
12. Peri, J. B., *J. Phys. Chem.* **86,** 1615 (1982).
13. Delgado, E., Fuentes, G. A., Hermann, C., Kunzmann, G., and Knozinger, H., *Bull. Soc. Chim. Belg.* **93,** 735 (1984).
14. Zaki, M. I., Vielhaber, B., and Knozinger, H., *J. Phys. Chem.* **90,** 3176 (1986).
15. Goldwasser, J., Fang, S. M., Houalla, M., and Hall, W. K., *J. Catal.* **115,** 34 (1989).
16. DeCanio, S. J., Cataldo, M. C., DeCanio, E. C., and Storm, D. A., *J. Catal.* **115,** 256 (1989).
17. Chung, J-S, Zhang, J. P., and Burwell, R. L., Jr., *J. Catal.* **116,** 506 (1989).
18. Yao, H. C., and Shelef, M., *J. Phys. Chem.* **78,** 2490 (1974).
19. Ratnasamy, P., and Knozinger, H., *J. Catal.* **54,** 155 (1978).
20. Bachelier, J., Tilliette, M. J., Cornac, M., Duchet, J. C., Lavalley, J. C., and Cornet, D., *Bull. Soc. Chim. Belg.* **93,** 743 (1984).
21. Topsøe, N-Y, and Topsøe, H., *J. Catal.* **75,** 354 (1982).
22. Wilson, T. P., Kasai, P. H., and Ellgen, P. C., *J. Catal.* **69,** 193 (1981).
23. van den Berg, F. G. A., Glezer, J. H. E., and Sachtler, W. M. H., *J. Catal.* **93,** 340 (1985).
24. Underwood, R. P., and Bell, A. T., *J. Catal.* **109,** 61 (1988).
25. Jen, H. W., Zheng, Y., Shriver, D. F., and Sachtler, W. M. H., *J. Catal.* **116,** 361 (1989).
26. Kip, B. J., Smeets, P. A. T., van Wolput, J. H. M. C., Zandbergen, H. W., van Grondelle, J., and Prins, R., *Appl. Catal.* **33,** 157 (1987).
27. Sudhakar, C., Bhore, N. A., Bischoff, K. B., Manogue, W. H., and Mills, G. A., *in* "Proceedings, 10th Meeting of Catalysis Society of North America, San Diego, CA, 1987."
28. Foley, H. C., Hong, A. J., Brinen, J. S., Allard, L. F., and Garratt-Reed, A. J., *Appl. Catal.* **61,** 351 (1990).
29. Hu, Z., Nakamura, H., Kunimori, K., Yokoyama, Y., Asano, H., Soma, M., and Uchijima, T., *J. Catal.* **119,** 33 (1989).
30. Ichikawa, M., and Fukushima, T., *J. Phys. Chem.* **89,** 1564 (1985).
31. Ichikawa, M., Lang, A. J., Shriver, D. F., and Sachtler, W. M. H., *J. Am. Chem. Soc.* **107,** 7216 (1985).
32. Fukushima, T., Arakawa, H., and Ichikawa, M., *J. Phys. Chem.* **89,** 4440 (1985).
33. Sachtler, W. M. H., and Ichikawa, M., *J. Phys. Chem.* **90,** 4752 (1986).
34. Dictor, R., and Roberts, S., *J. Phys. Chem.* **93,** 5846 (1989).
35. Foley, H. C., DeCanio, S. J., Tau, K. D., Chao, K. J., Onuferko, J. H., Dybowski, C., and Gates, B. C., *J. Am. Chem. Soc.* **105,** 3074 (1983).
36. Blackmond, D. G., Williams, J. A., Kesraoui, S., and Blazewick, D. S., *J. Catal.* **101,** 496 (1986).
37. Kesraoui, S., Oukaci, R., and Blackmond, D. G., *J. Catal.* **105,** 432 (1987).
38. Angevaare, P. A. J. M., Hendrickx, H. A. C. M., and Ponec, V., *J. Catal.* **110,** 11 (1988).
39. Uram, K. J., Lily, Ng, Folman, M., and Yates, J. T., Jr., *J. Chem. Phys.* **84,** 2891 (1986).
40. Solymosi, F., Pasztor, M., and Rakhely, G. Ra, *J. Catal.* **110,** 413 (1988).